Nonlinear conductance in finite-length armchair single-wall carbon nanotubes with one single impurity

2008 J. Phys.: Condens. Matter 20 135213

(http://iopscience.iop.org/0953-8984/20/13/135213)

IOP PUBLISHING JOURNAL OF PHYSICS: CONDENSED MATTER

J. Phys.: Condens. Matter **20** (2008) 135213 (8pp) doi:10.1088/0953-8984/20/13/135213

Nonlinear conductance in finite-length armchair single-wall carbon nanotubes with one single impurity

Pouya Partovi-Azar[1] **and Afshin Namiranian**[1,2]

[1] Department of Physics, Iran University of Science and Technology, Narmak, 16345, Tehran, Iran
[2] Computational Physical Science Laboratory, Department of Nano-Science, Institute for Studies in Theoretical Physics and Mathematics (IPM), PO Box 19395-5531, Tehran, Iran

E-mail: p.partovi@physics.iust.ac.ir and afshinn@iust.ac.ir

Received 2 November 2007, in final form 31 January 2008
Published 12 March 2008
Online at stacks.iop.org/JPhysCM/20/135213

Abstract

We investigate theoretically the nonlinear quantum conductance of finite single-wall carbon nanotubes (SWCNTs) due to the presence of a single impurity. To take the length of the tube into account and retain the periodicity of the SWCNT along its axis, a particle-in-a-box model is employed. The dependence of the differential conductance on the gate voltage as well as its sensitive dependence on the position of the possible impurity in the tube is studied. Results suggest a promising method for spectroscopy of electronic energy levels in a SWCNT.

1. Introduction

Nowadays, great developments in experimental methods have produced a gleam of hope of using carbon nanotubes in electrical devices [1, 2]. The ability of using carbon nanotubes in such devices will open a door to a wide range of applications for these structures. A single-wall carbon nanotube (SWCNT) can be considered as a graphene sheet folded around a specific axis. Depending on the properties of this axis and the radius of the tube, a SWCNT shows its own electrical properties. Almost one third of these structures are conductors [3, 4].

Ideal metallic SWCNTs in the ballistic regime are categorized as quantum conductors [5]. In a quantum conductor, on the basis of Landauer theory [6], conductance is quantized. The conductance of an ideal SWCNT is $G_0 = 4e^2/h$ [7] (and references therein). Meanwhile, the presence of any kind of disorder or imperfection in these structures will affect the conductance [8, 9]. These disorders are always present: phonons [10]; defects at the points of connection between nanotubes and contact electrodes [11, 12]; common structural defects in nanotubes such as Stone–Wales defects [13, 14]; and even desirable or undesirable non-carbon atoms on the surface of the tube [15–17].

In the last case, unlike for the bulk conductors, the presence of a single impurity will dramatically change the conductance. The more interesting point is that the conductance is not only dependent on the number of such single defects, but also on their positions. This is what results in negative differential conductance or quantum interference. These phenomena were the subject of some of our studies [18, 19] as well as those of others [20–24].

Using well-known techniques [25], now researchers are able to cut nanotubes into segments of length of a few tens of nanometers. This produces new electronic properties for finite-length carbon nanotubes: confinement of the length results in completely quantized energies for conduction electrons—confirmed by experiment [26, 27]—and leads to the probability of finding electrons being different from one point to another along the nanotube, which is essential in understanding the size effects. Obviously, it is important to study such quantum size effects in view of the device application of nanotubes. Different studies have already focused on electronic properties of finite-length carbon nanotubes [28–30].

In this research we are going to deal with only one single impurity (or defect) on the surface of a finite metallic SWCNT. We tried to analytically obtain the change in the conductance of a SWCNT, due to the presence of a single defect, by means of a very simple model for including tube length, based on a perturbative scheme. As will be expressed, for a limited length carbon nanotube, the amount of scattering of the conduction electrons' wavefunctions from a defect (and as a result the change in the conductance of the nanotube) depends on the

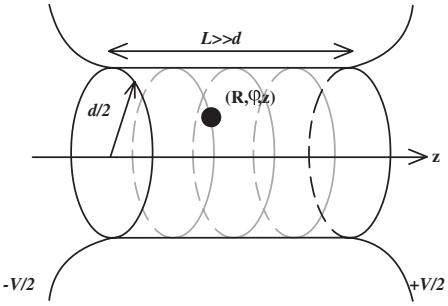

Figure 1. The model of a SWCNT in the form of a long cylindrical surface of the diameter d, which smoothly connects two massive metallic reservoirs. The impurity or defect on the surface of the cylinder is shown schematically.

position of the possible defect. We have tried to investigate this dependence as well as the nonlinear part of the conductance. We see that our results introduce a quantitative method for spectroscopy of the energy levels as well as imaging the probability distribution of conduction electrons. This is what can be investigated by nanoprobes as a cause of such point-like defects.

Thus this paper is organized as follows. In section 2, we introduce a method for calculating the change in conductance in a SWCNT due to the presence of one single defect; in section 3, our model for obtaining the wavefunctions as well as energy levels for conduction electrons in a finite-length SWCNT is introduced. In section 4, we discuss observed dependences in results obtained. And finally we end with a conclusion.

2. Method of calculation of the differential conductance

Let us consider a metallic SWCNT as a long but finite cylinder, which connects two bulk metallic electrodes. The electrodes lie at different voltages V, assuming $eV \ll E_F$. We also assume that a single impurity (or defect) is located on the surface of the cylinder (as shown in figure 1).

We will completely neglect possible backscattering of electrons on metal contacts. The Hamiltonian of the electrons, H, contains the following terms:

$$H = H_0 + H_1 + H_{\text{int}} \tag{1}$$

where

$$H_0 = \sum_k \varepsilon_k c_k^\dagger c_k \tag{2}$$

is the Hamiltonian of Bloch electrons 'feeling' only the perfect lattice of SWCNT,

$$H_1 = \frac{eV}{2} \sum_k \text{sgn}(v_z) c_k^\dagger c_k \tag{3}$$

describes the interaction of the electrons with the electric field. Here operator ${c_k}^\dagger$ (c_k) creates (annihilates) a conduction electron with wavefunction Ψ_k and energy ε_k. As will be seen later, k is the full set of electron quantum numbers for translational and rotational degrees of freedom (ignoring spin). v_z is the electron velocity along the tube axis. Finally H_{int} is the Hamiltonian of interaction between electrons and the impurity:

$$H_{\text{int}} = \sum_{k,k'} \mathbf{J}_{k,k'} c_k^\dagger c_{k'} \tag{4}$$

where in general

$$\mathbf{J}_{k,k'} = \int \mathrm{d}\mathbf{r} J(\mathbf{r}) \Psi_k(\mathbf{r}) \Psi_{k'}^*(\mathbf{r}). \tag{5}$$

The strength of this interaction is assumed to be small. The conductance of the system is described by the Landauer formula, which is applicable if the wavefunction can spread over the whole sample. In order to investigate the influence of the defect, a perturbative scheme along with the second-quantized representation of the Hamiltonian can be used. The change in the electrical current ΔI is related to the rate of energy dissipation by the relation

$$\Delta I V = \frac{\mathrm{d}E}{\mathrm{d}t} = \frac{\mathrm{d}\langle H_1 \rangle}{\mathrm{d}t}. \tag{6}$$

The differential of $\langle H_1 \rangle$ with respect to time t is obtained from the Heisenberg equation. The change ΔI of the current due to interactions of electrons with impurities would then be

$$\Delta I V = \frac{1}{\mathrm{i}\hbar} \langle [H_1(t), H_{\text{int}}(t)] \rangle, \tag{7}$$

where

$$\langle O \rangle = \text{Tr}\left[\rho(t)\, O\right]. \tag{8}$$

All operators are in the interaction representation.

The statistical operator $\rho(t)$ satisfies the equation

$$\mathrm{i}\hbar \frac{\partial \rho}{\partial t} = [H_{\text{int}}(t), \rho(t)] \tag{9}$$

which can be solved using perturbation theory in H_{int} (but for arbitrary H_1). Thus, the change in the electric current due to the presence of impurity can be written as [31, 32]

$$\begin{aligned} \Delta I &= I_1 + \cdots \\ &= -\frac{1}{\hbar^2 V} \int_{-\infty}^{t} \mathrm{d}t' \,\text{Tr}\left(\rho_0 \left[[H_1, H_{\text{int}}(t)], H_{\text{int}}(t')\right]\right) + \cdots \end{aligned} \tag{10}$$

where ρ_0 is the statistical operator for the electrons. Then the first-order correction to the current would be

$$\begin{aligned} I_1 = -\frac{e\pi}{\hbar} \sum_{n,m} &(\text{sgn}\, v_{z_m} - \text{sgn}\, v_{z_n})(f_m - f_n) \\ &\times \delta(\varepsilon_n - \varepsilon_m) \mathbf{J}_{n,m}. \end{aligned} \tag{11}$$

Here $f_n = f_{\text{FD}}[\varepsilon_n + (eV/2)\text{sgn}(v_z)]$ is a function of voltage. Recalling the definition of $\mathbf{J}$, from the above equation it is clear that the current I_1 depends on the value of the electronic wavefunctions at the point where the defect is situated. This is totally a quantum effect. We assume that the interaction is point-like,

$$J(\mathbf{r}) = g\delta(\mathbf{r}), \tag{12}$$

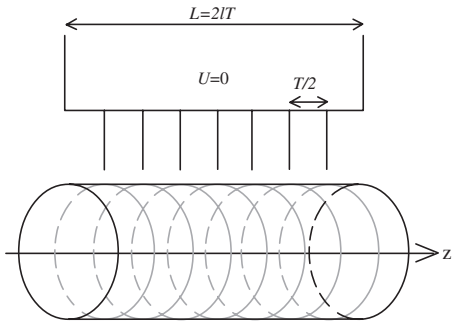

Figure 2. Schematically showing the geometry of the particle-in-a-box model for finite carbon nanotubes as well as corresponding perturbative potential. The translational period for SWCNTs along the tube axis is T.

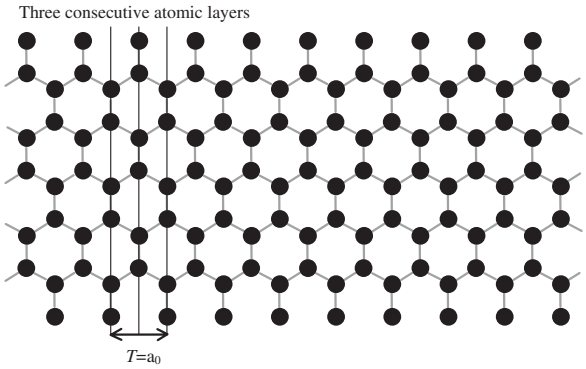

Figure 3. Unfolded armchair SWCNT. The vertical axis is along the circumference and the horizontal axis is along the tube axis (z-axis). The translational period of the tube is shown in the figure. Three consecutive atomic layers are also depicted. As is clear, there are equal numbers of carbon atoms in every atomic layer.

and we work at zero temperature. At zero temperature, $f_n = \Theta[E_F - \varepsilon_n - (eV/2)\mathrm{sgn}(v_z)]$ is the Heaviside step function. By differentiating equation (11) over the gate voltage, we would obtain the conductance due to the presence of the impurity G_1 as [33, 18]

$$G_1 = G_0 \left(\frac{g\pi}{2}\right)^2 \sum_{m,n} (\mathrm{sgn}\, v_{z_m} \mathrm{sgn}\, v_{z_n} - 1) \times \delta\left(E_F - \varepsilon_n - \frac{eV}{2}\mathrm{sgn}\, v_{z_n}\right) \times \delta(\varepsilon_n - \varepsilon_m)\,[\Psi_m^2(\mathbf{r})\Psi_n^2(\mathbf{r})]. \quad (13)$$

At this point, all the results within the perturbation theory are exact. To illustrate the result, one should use the wavefunctions and energy spectrum for conducting Bloch electrons in SWCNTs.

3. Wavefunctions and energies: particle-in-a-box model

The tight-binding method for graphene sheet, along with the zone-folding approximation, is the most common method for calculating the wavefunctions and energies for infinitely long SWCNTs [34–36]. Several methods have been already presented for obtaining the wavefunctions as well as energies for finite SWCNTs [37–41].

In order to calculate the energy spectrum and wavefunctions of Bloch electrons we consider a simple model for nanotubes here. We assume that we are dealing with long but finite-length particle-in-a-box form. To impose the periodic structure of SWCNTs along the tube axis, which is set to be in the z-direction, we assume that the electron moving along the tube axis has a Hamiltonian of the form

$$H_0 = \frac{P^2}{2m} + U, \qquad U = c\sum_{q=1}^{2l-1} \delta(z - qT/2) \qquad 0 < z < l \quad (14)$$

where c is strength of the δ-potential with the dimension of energy $\times$ length, z is along the tube axis and T is the translational period of the tube along its axis. $2l$ shows the length of the tube in units of translational period along the tube axis T, where for armchair tubes $T = a_0 = 2.461$ Å and for zigzag tubes $T = \sqrt{3}a_0$ Å. a_0 is the length of the basis vectors of the graphene honeycomb lattice and the carbon–carbon bond length is assumed to be $a_{cc} = 1.421$ Å [42]. The tube length is then $2lT$. More importantly this term keeps the periodicity needed for taking the structure of the nanotube into account. Figure 2 shows the potential term.

Now let us consider the armchair tubes. Here we have modeled the effect of each of the atomic layers, which are placed at every $qT/2$ for $q = 1, 2, \ldots, 2l - 1$ along the tube axis, with an attractive δ-potential ($c < 0$) of the same strength. Assuming the same strength for all δ-potentials is reasonable since in armchair tubes there are equal number of carbon atoms in every atomic layer. Figure 3 shows an unfolded armchair SWCNT. The vertical axis is along the circumference of the tube while the horizontal axis is along the tube axis (z-axis).

As is clear, the above Hamiltonian is totally one dimensional. This approximation will be valid only for those tubes with large ratio of length to diameter. This is essentially the case for practical use in many application in nanoelectronics. The more accurate model has already been presented by considering the tube as a three-dimensional molecule and approximating the $2p_z$ orbital of each carbon atom with such attractive δ-potential [43]. The strength of the δ-potential here is indeed different from what the authors have presented in [43]. They have regularized the strength by fitting with *ab initio* and tight-binding results.

The Hamiltonian (14) has an exact solution for its wavefunctions and energies which can be found by elementary quantum mechanics methods. Basically, such a solution for wavefunctions has $2l$ parts for which every solution is valid for a particular partition (say the ith partition: $iT/2 \leqslant z < (i + 1)T/2$). Each corresponding energy level would then be found from a transcendental equation either by a graphical method or by numerical calculations. Since equation (13) requires wavefunctions and energies for every quantum level, to continue more analytically, we will follow a perturbation scheme as an alternative method. Perturbation then provides us with nicer relations for wavefunctions as well as energies.

Besides the kinetic energy term in equation (14), what remains can be considered as a perturbation potential for a particle-in-a-box system. The wavefunctions for the system to the first-order correction would be of the form

$$\Psi_{r,s}(z,\phi) = \left[\sin\left(\frac{r\pi z}{l}\right) + \left(\frac{2}{l}\right)cl^2 \times \sum_{m\neq r}\sum_{q=1}^{2l-1}\left(\frac{1}{r^2-m^2}\right)\sin\left(\frac{m\pi q}{2l}\right)\sin\left(\frac{r\pi q}{2l}\right) \times \sin\left(\frac{m\pi z}{l}\right)\right] \times \left(\sqrt{\frac{2}{\pi dl}}\right)\exp(\mathrm{i}s\phi)\,. \quad (15)$$

The corresponding energies for the translational degree of freedom to the first-order correction take the form

$$\epsilon_r{}^{\mathrm{trans}} = \left(\frac{r^2}{l^2}\right) + c\left(\frac{2}{l}\right)\sum_{q=1}^{2l-1}\sin^2\left(\frac{r\pi q}{2l}\right) \quad (16)$$

in terms of $E_0 = \pi^2\hbar^2/2mT^2$ and $r = 1, 2, 3, \ldots$.

It should also be emphasized that the perturbative potential employed here has nothing to do with rotational degree of freedom for electrons. This is why the first correction to the energy is independent of quantum number s.

In equations (15) and (16), lengths and energies are written respectively in units of T and E_0. The first two wavefunctions corresponding to two lowest energies as a function of z in the direction of the tube axis are shown in figure 4 for an armchair SWCNT of length $25T$ $(=a_0)$. Obviously, these wavefunctions consist of two factors: a periodic function retaining the periodicity of the nanotube structure; and a particle-in-a-box wavefunction. What is experimentally seen by STM imaging is just a superposition of these electronic wavefunctions near the Fermi level. This is consistent with the STM imaging done experimentally by Venema *et al* [44]. The point that should be kept in mind is that as the length of the tube is increased, small oscillations lose their amplitude. Figure 4 is just plotted to show the behavior of corrected wavefunctions while a tube with length $25a_0$ cannot be *accurately* described with this model (since, as stated earlier, this model is more suitable for tubes with large ratio of length to diameter). In figure 4, the strength of the δ-potentials was fixed in such a way that the ground state (GS) energies of our model and the tight binding are equal.

For armchair tubes we have $T = a_0$ and therefore $E_0 = \pi^2\hbar^2/2ma_0{}^2$. The total number of carbon atoms in the unit cell of a nanotube is [42]

$$n_{\mathrm{c}} = \frac{4\left(n_1{}^2 + n_1n_2 + n_2{}^2\right)}{nR} \quad (17)$$

where n_1 and n_2 are indices of the tube which for armchair tubes are the same; n is the greatest common divisor of n_1 and n_2. Each carbon atom contributes only one electron (a $2\mathrm{p}_z$ orbital electron) to the total conductance. These are the electrons that will occupy the energy levels of a particle-in-a-box model. The other three electrons $((\mathrm{sp}^2)_1$, $(\mathrm{sp}^2)_2$ and $(\mathrm{sp}^2)_3)$ are well bound to the carbon atom's nucleus. For armchair nanotubes $R = 3$, so the total number of $2\mathrm{p}_z$ orbital electrons in an armchair tube will be $N = 4nl$.

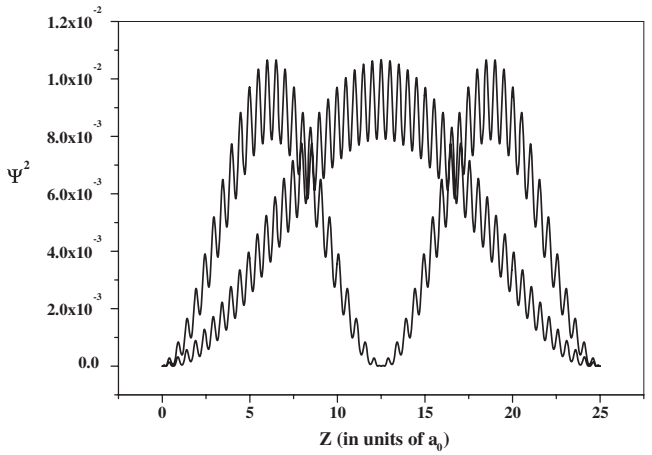

Figure 4. Squared electronic wavefunctions corresponding to two lowest energies for an armchair (5, 5) SWCNT of length $25a_0$. The perturbation constant, c, is set in such a way that the ground state (GS) energy of our simple model and the GS energy in nearest-neighbor TB are equal. The wavefunctions consist of two factors: a particle-in-a-box wavefunction; and a periodic function (small oscillations in the figure) which retains the periodicity of the tube along its axis.

The diameter of a nanotube is given by

$$d = \frac{a_0}{\pi}\sqrt{n_1{}^2 + n_1n_2 + n_2{}^2} \quad (18)$$

so the discrete energy levels for rotational degree of freedom for an armchair SWCNT in our simple model are given by

$$\epsilon_s{}^{\mathrm{rot}} = \frac{4}{3}\left(\frac{s}{n}\right)^2 \quad (19)$$

in terms of E_0 and $s = 0, 1, 2, \ldots$. In fact, the quantity $\varepsilon_{r,s} = \epsilon_r{}^{\mathrm{trans}} + \epsilon_s{}^{\mathrm{rot}}$ is just ε_k which was introduced in equation (2).

A discussion on the Fermi energy is needed here. The energy levels of the system, as introduced above, are given by $\varepsilon_{r,s} = \epsilon_r{}^{\mathrm{trans}} + \epsilon_s{}^{\mathrm{rot}}$. To find a value for the Fermi energy, all we should do is to distribute N conduction electrons to a pair of quantum numbers (r, s) (each quantum state denoted by the pair (r, s) accepts two electrons, including spin) and find the minimum of the possible values for $\varepsilon_{r,s}$. In general, the Fermi energy would then be a function of the tube length as well. Figure 5 shows the Fermi energy as a function of the tube length. As the length of the tube increases, the Fermi energy approaches a constant value. The constant value that the Fermi energy eventually reaches, comes from distributing all N conduction electrons to energy levels corresponding only to translational degrees of freedom introduced in equation (16). Including spin, the Fermi energy would be of the form $E_{\mathrm{F}} \approx (N/2l)^2$, in units of E_0, where N is the total number of $2\mathrm{p}_z$ orbital electrons in the tube. By inserting N into E_{F} we get

$$E_{\mathrm{F}} \approx (2n)^2 \quad (20)$$

which is obviously independent of tube length. n denotes the tube index. The dependence of the Fermi energy on the length is totally a result of confining the length of the tube.

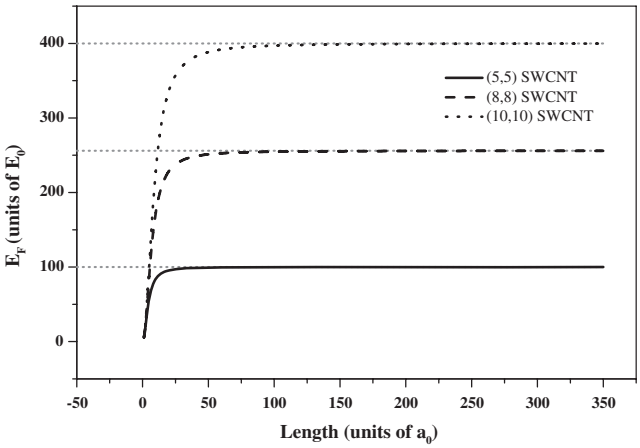

Figure 5. Fermi energy (in units of E_0) versus length for armchair SWCNTs with different diameters. For short tubes, the Fermi energy sensitively depends on the length of the tube. The Fermi energy rapidly rises and finally reaches a constant value, $(2n)^2$, for each case. Each curve corresponds to SWCNTs with different diameter.

This feature cannot be seen in infinite SWCNTs [44]. The difference between the more exact value for the Fermi energy and equation (20) becomes greater for a fixed-length tube as the diameter increases. We also see that the value of the Fermi energy for the tubes with lengths longer than $100a_0$ is nearly independent of length for all diameters shown in the figure. To use the length-independent form for the Fermi energy (equation (20)), we consider armchair SWCNTs with lengths longer than $100a_0$ hereafter.

Since we are dealing with squared wavefunctions and we have a single defect in the problem (see equation (13)), assuming the plane wave form for the wavefunctions of electrons in their rotational degree of freedom shows that we can easily neglect the electron's wavefunctions for its rotational degree of freedom in this simple model. In fact, this is one of the points that can be revised by using a more realistic model.

Now we are well equipped to provide equation (13) with wavefunctions as well as discrete energies of electrons.

4. Results and discussion

In the present section, we show the results from figures 6–8. The vertical axis in the figures is scaled in such a way that we have $(\frac{gm_e}{\pi\hbar^2})^2 \times 10^{-4} = 1$. In figure 6 we have plotted the change in conductance due to the presence of a single defect versus gate voltage (V). The gate voltage has been set to $0.01E_F$ to $0.1E_F$ in each case. Figure 6(a) shows G_1 for a (10, 10) SWCNT of length $150\ a_0$. As was shown before in figure 5, in this case we can use the length-independent form for the Fermi energy with a good approximation. To see the effect of length-dependent Fermi energy, we have plotted the same graph in figure 6(b) but this time for a (10, 10) SWCNT of length $50a_0$. In both figures 6(a) and (b) G_1 sensitively depends on gate voltage and some oscillatory patterns are also observed. The patterns in figures 6(a) and (b) are almost the same for different graphs which correspond to different positions of the defect on the tube.

If we go back to equation (13), we see that gate voltage (V) controls the contribution of conduction electrons to the total conductance in this way: let us say an electron which contributes to the total differential conductance has an arbitrary energy E_{arb}. Then E_{arb} differs from E_F just by the value of V. If the difference between E_{arb} and E_F is more or less than V, then the electron with energy E_{arb} cannot contribute to the total differential conductance.

The index and the length of the nanotube is fixed in figure 6(a). So, the energy spectrum is not changed for different curves in figure 6(a). The observation of a peak in G_1, for example around $0.025E_F$, in all three curves in figure 6(a) shows that the number of states with difference in energy around $0.025E_F$ from the Fermi energy is larger compared to that of states with difference in energy say around $0.03E_F$ from E_F. This can be considered as some kind of spectroscopy. This

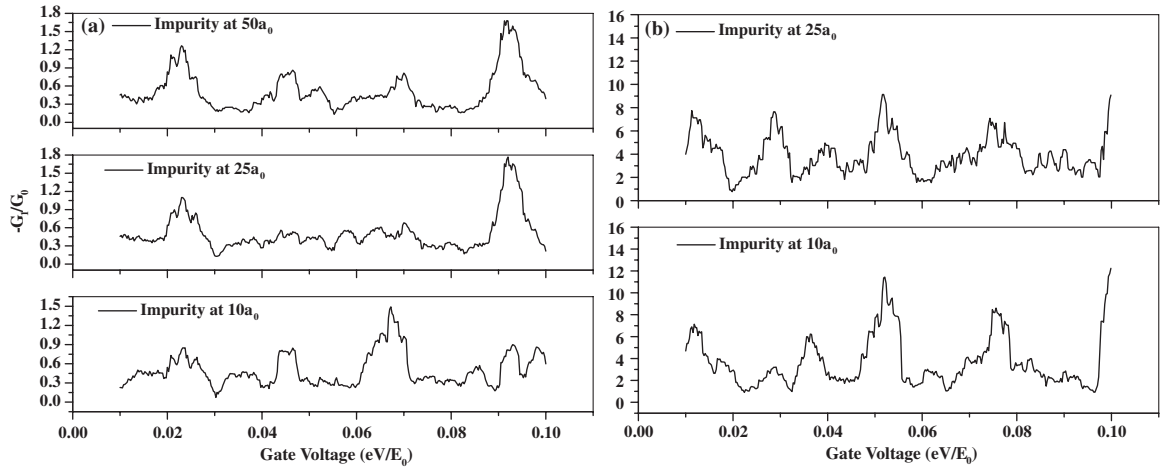

Figure 6. First correction to the conductance versus gate voltage for a (10, 10) SWCNT of length (a) $150a_0$ and (b) $50a_0$. In the case of (a), E_F is independent of the tube length (see figure 5) but in (b) we have used the more exact Fermi energy. Each curve corresponds to different positions of the defect on the tube. The gate voltage varies from 0.01 to $0.1E_F$ in each case. (a) shows that the number of states with difference in energy around $0.025E_F$ from the Fermi energy are larger in comparison with say $0.03E_F$. This is also true in (b) for states with energy difference around $0.1E_F$ from the Fermi energy.

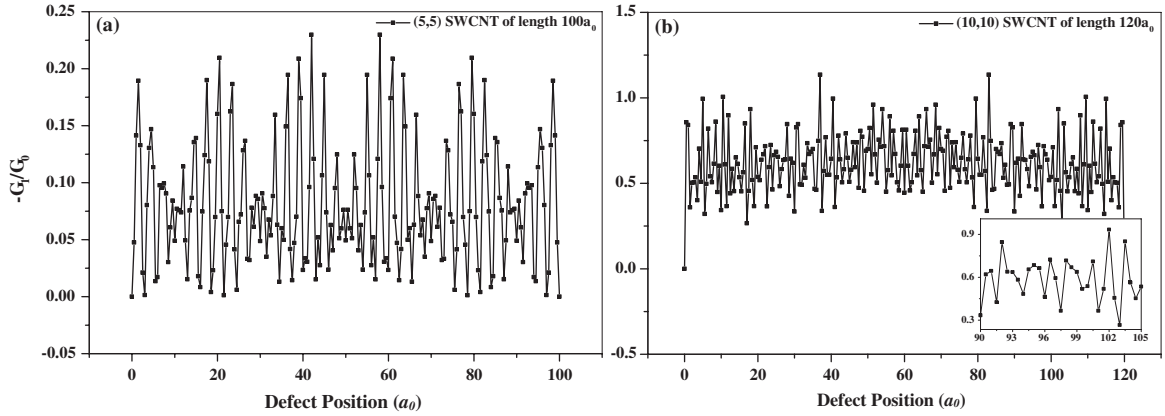

Figure 7. First correction to the conductance versus position of the defect along the tube axis for (a) (5, 5) and (b) (10, 10) SWCNTs respectively of length $100a_0$ and $120a_0$. The gate voltage is set to $0.01E_F$.

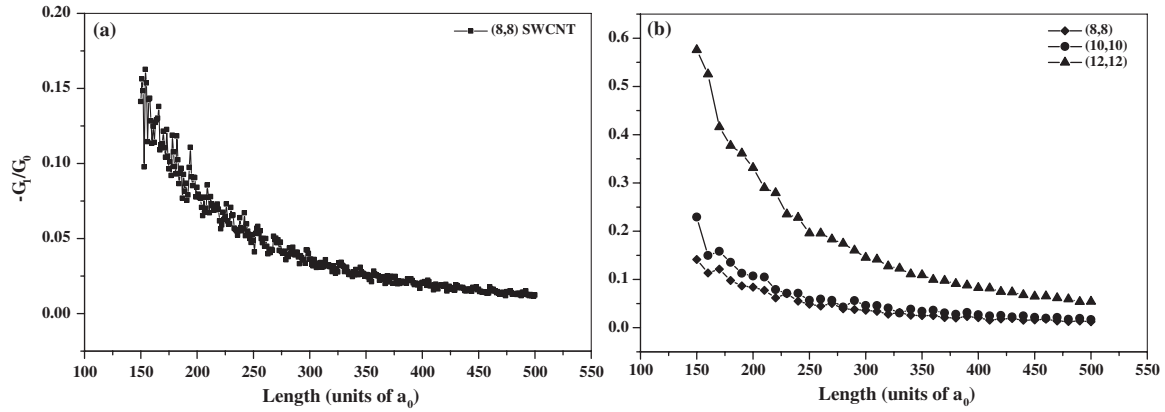

Figure 8. First correction to the conductance versus length of the tube. Positions of the defects are similar for all curves in (a) and (b). The defect is situated at $10a_0$. (a) shows a rapidly decreasing behavior of the correction to the conductance versus length of the tube for a (8, 8) SWCNT. In (b), this behavior is studied when the tube diameter is changed. As the diameter grows larger, the first correction increases in value. The gate voltage is set to $0.01E_F$ in both (a) and (b).

feature is more obvious in figure 6(b). The energy spectrum is similar for different curves in figure 6(b), yet different from figure 6(a) since the length of the tube in figure 6(b) is different from the tube length in figure 6(a).

The overall value for G_1 in figure 6(a) is much less than that for figure 6(b). This is the case because the interaction of electrons in shorter tubes with the defect is greater. We can say that the spatial distribution of electronic wavefunctions in shorter tubes is confined to a shorter particle-in-a-box system. For tubes with the same diameter, shortening the length also results in greater amplitude of all electronic wavefunctions (see equation (15)). In this way, for a fixed defect, the sum of all squared electronic wavefunctions near the Fermi level at the position of the defect is greater in comparison with the longer tube case. In other words, for the case of shorter tubes, the presence of the defect is more appreciable for conduction electrons. So, G_1 is then greater for shorter tubes.

Moreover, the pattern in figure 6(a) is more complicated than the pattern in figure 6(b). This can be understood by counting the number of available electronic energies and corresponding wavefunctions which contribute to the total amount of G_1. Recall that for shorter nanotubes, the distances between energy levels are larger, which results in a smaller number of states around the Fermi energy. Consequently the total sum in equation (4) consists of the superposition of fewer wavefunctions leading to less complication for shorter nanotubes comparing to larger ones.

In figures 7(a) and (b), G_1 is plotted versus the position of the defect respectively for (5, 5) and (10, 10) armchair SWCNTs. The lengths of the tubes in figures 7(a) and (b) are respectively $100a_0$ and $120a_0$. This shows that the differential conductance sensitively depends on the defect position along the tube and has an oscillatory pattern.

To discuss this, let us go back once again to equation (13). It is clear that G_1 depends on the values of squared electronic wavefunctions, corresponding to all quantum numbers which satisfy the two δ-functions in the equation, at the point at which the defect is placed. So, as was stated before, G_1 is a measure of all squared electronic wavefunctions that contribute to the conduction of the tube. The value of G_1 at a point in figures 7(a) and (b) is just the sum of all squared electronic wavefunctions near the Fermi level at that point. The sensitive dependence of G_1 on the position of the defect is then reasonable.

In addition, it is clear that the graph is symmetric with respect to the middle point of the tube: $50a_0$ in figure 7(a), and $60a_0$ in figure 7(b). Since the wavefunctions of electrons in our model are symmetric with respect to the middle of the tube (see figure 4), the G_1 graph should also be symmetric with respect to the same point. Another feature is that since the wavefunctions of electrons vanish at the two ends of the tube (due to the particle-in-a-box model), G_1 also vanishes at these points, as expected. It is also seen that the first correction to the conductance for a (10, 10) SWCNT (figure 7(b)) is considerably larger than that of a (5, 5) SWCNT (figure 7(a)).

In figure 7(b) we have plotted the G_1 graph for a (10, 10) SWCNT of length $120a_0$. This tube is almost the same in length and diameter as the one that was the subject of experimental investigations by Venema *et al* [44]. Here we should state that comparison between figure 7(b) and results given by Venema *et al* is meaningful: changing the position of the defect along the axis of the tube and calculating the differential conductance using equation (13) is qualitatively similar to imaging the squared electronic wavefunctions through the nanotube. They used a tube of length 300 nm and diameter 1.4 nm. Our very simple model shows a wavelength that agrees with experimental results with an acceptable difference. The experimentally reported wavelength is $\approx 3a_0$ while our calculations suggest almost the same value (see the inset of figure 7(b); since we have a measure for squared electronic wavefunctions, we should consider two consecutive peaks).

Figure 8 shows the behavior of the differential conductance versus the length of the tube while the defect is situated at a fixed position. The descending behavior of the nonlinear conductance can be described as follows: as the length of the nanotube is increased, the number of carbon atoms (as well as conduction electrons) is also increased. So, we eventually reach the thermodynamic limit. In these conditions, the effect of a single defect as a scattering center for electrons can easily be neglected. It is clear that the effect of a single defect on the conductance cannot be seen in infinite tubes.

A common feature in the figures 7 and 8(b) is that on increasing the diameter of the tube, the first correction to the conductance rises. For example, compare the overall value for the first correction to the conduction in figures 7(a) and (b); or see figure 8(b). This is because in tubes with larger diameter (yet with the same length) there are more modes available for conduction electrons to move along the tube. So, interaction of electrons with the defect would then be greater and this increases the absolute value of the correction to the conductance.

5. Conclusion

In conclusion, the effect of a single defect on the differential conductance of a finite-length armchair single-wall carbon nanotube within the context of a perturbation scheme is studied by using a simple model. Our results show that there is an interplay between the position of the defect, the length and the diameter of the tube which affect the value of the differential conductance. For a nanotube with fixed length and diameter and a defect positioned at a fixed point, the nonlinear differential conductance shows a non-monotonic behavior as a function of gate voltage, having some local maxima whose distances are related to the electronic energy level spacing of the nanotube. This shows a potential application of a new spectroscopy method for electronic energy levels in metallic SWCNTs.

Also our results show that while the position of the defect changes smoothly over the surface of a finite-length nanotube, differential conductance has an oscillatory behavior. The period of such oscillations does not depend on the defect position and only depends on the length and the diameter (and consequently the electronic energy spectrum) of the nanotube. Moreover this study, as is expected, shows that the differential conductance decreases rapidly as the length of the SWCNTs is increased.

References

[1] Javey A, Guo J, Wang Q, Lundstrom M and Dai H 2003 *Nature* **424** 654
[2] Appenzeller J, Knoch J, Radosavlievic M and Avouris Ph 2004 *Phys. Rev. Lett.* **92** 226802
[3] Hamada N, Sawada S I and Oshiyama A 1992 *Phys. Rev. Lett.* **68** 1579
[4] Mintmire W, Dunlap B I and White C T 1992 *Phys. Rev. Lett.* **68** 631
[5] Liang W, Bockrath M, Bozovic D, Hafner J H, Tinkham M and Park H 2001 *Nature* **411** 665
[6] Landauer R 1970 *Phil. Mag.* **21** 863
[7] Frank S, Poncharal P, Wang Z L and de Heer W A 1998 *Science* **280** 1744
[8] Charlier J Ch, Blase X and Roche S 2007 *Rev. Mod. Phys.* **79** 677
[9] Yao Z, Postma H W C, Balents L and Dekker C 1999 *Nature* **402** 273
[10] Roche S, Jiang J, Foa Torres L E F and Saito R 2007 *J. Phys.: Condens. Matter* **19** 183203
[11] Tersoff J 1999 *Appl. Phys. Lett.* **74** 2122
[12] Andriotis A N and Menon M 2007 *Phys. Rev.* B **76** 045412
[13] Stone A J and Wales D J 1986 *Chem. Phys. Lett.* **128** 501
[14] He Y, Zhang Ch, Cao Ch and Cheng H P 2007 *Phys. Rev.* B **75** 235429
[15] Liu Y and Guo H 2004 *Phys. Rev.* B **69** 115401
[16] Park J Y 2007 *Appl. Phys. Lett.* **90** 023112
[17] Bockrath M, Liang W, Bozovic D, Hafner J H, Lieber Ch M, Tinkham M and Park H 2001 *Science* **291** 283
[18] Namiranian A 2004 *Phys. Rev.* B **70** 073402
[19] Bagheri M and Namiranian A 2007 *J. Phys.: Condens. Matter* **19** 096207
[20] Zhang Q, Yang H and Ma Zh 2006 *Phys. Rev.* B **73** 235438
[21] Farajian A A, Esfarjani K and Kawazoe Y 1999 *Phys. Rev. Lett.* **82** 5084
[22] Maksimenko A S and Slepyan G Ya 2000 *Phys. Rev. Lett.* **84** 362
[23] Rochefort S and Avouris Ph 2000 *J. Phys. Chem.* A **104** 9807
[24] Song H F, Zhu J L and Xiong J J 2002 *Phys. Rev.* B **66** 245421
[25] Venema L C, Wildoer J W G, Temminck Tuinstra H L J, Dekker C, Rinzler A G and Smalley R E 1997 *Appl. Phys. Lett.* **71** 2629
[26] Bockrath M, Codben D H, McEuen P L, Chopra N G, Zettl A, Thess A and Smalley R E 1997 *Science* **275** 1922
[27] Tans S J, Devoret M H, Dai H, Thess A, Smalley R E, Geerligs L S and Dekker C 1997 *Nature* **386** 474
[28] Rochefort A, Salahub D R and Avouris Ph 1999 *J. Phys. Chem.* B **103** 641

[29] de Pablo P S, Gomez-Navarro C, Colchero J, Serena P A, Gomez-Herrero J and Baro A M 2002 *Phys. Rev. Lett.* **88** 036804
[30] Orlikowski D, Mehrez H, Taylor J, Guo H, Wang J and Roland Ch 2001 *Phys. Rev.* B **63** 155412
[31] Kulik I O 1967 *JETP Lett.* **5** 345
[32] Kulik I O, Omelyanchouk A N and Tuluzov I G 1988 *Sov. J. Low Temp. Phys.* **14** 149 (Russian Language; page number for English translation of this article is 82)
[33] Namiranian A, Kolesnichenko Yu A and Omelyanchouk A N 2000 *Phys. Rev.* B **61** 16796
[34] Saito R, Dresselhaus G and Dresselhaus M S 1998 *Physical Properties of Carbon Nanotubes* (London: Imperial)
[35] White C T and Mintmire J W 1998 *Nature* **394** 29
[36] Reich S, Maultzsch J, Thomsen C and Ordejón P 2002 *Phys. Rev.* B **66** 035412
[37] Rubio A, Sanchez-Portal D, Artacho E, Ordejón P and Soler J M 1999 *Phys. Rev. Lett.* **82** 3520
[38] Jiang J and Xing D Y 2002 *Phys. Rev.* B **65** 245418
[39] Wu J, Duan W, Gu B L, Yu J Zh and Kawazoe Y 2000 *Appl. Phys. Lett.* **77** 2554
[40] Compernolle S, Chibotaru L and Ceulemans A 2003 *J. Chem. Phys.* **119** 2854
[41] Zhang Li Y 2002 *Chem. Phys. Lett.* **364** 328
[42] Reich S, Thomsen C and Maultzsch J 2004 *Carbon Nanotubes: Basic Concepts and Physical Properties* (New York: Wiley–VCH)
[43] Hsu H and Reichl L E 2005 *Phys. Rev.* B **72** 155413
[44] Venema L C, Wildoer J W G, Janssen J W, Tans S J, Temminck Tuinstra H L J, Kouwenhoven L P and Dekker C 1999 *Science* **283** 52